VARIATIONS OF THE MID-LATITUDINAL IONOSPHERE DRIVEN BY SPACE WEATHER.

BY

CHIAHA SHEDRACH OBUMNEME

UP202308817

A MONOGRAGH SUBMITTED TO THE UNIVERSTY OF MINHO/AVEIRO/PORTO, DEPARTMENT OF PHYSICS, PORTUGAL IN FUFILLMENT OF THE PHD ESSAY CURRICULUM UNIT.

SUPERVISORS:

ANNA MOROZOVA, UNIVERSITY OF COIMBRA.

TERESA BARATA, UNIVERSITY OF COIMBRA.

JOÃO LIMA, UNIVERSITY OF PORTO.

APRIL 2025

TABLE OF CONTENTS

LIST OF FIGURES

LIST OF TABLES

CHAPTER ONE

GENERAL INTRODUCTION

1.1 Sun and Solar wind

The energy driving the Geospace processes has its fundamental origin in the sun's core. Because of the high temperatures on and within the sun, the gas is ionized. An atom or molecule becomes ionized when an electron is knocked out, giving the atom a net positive electric charge. The charged particles feel the force of electric and magnetic fields. In addition, moving charged particles can create an electrical current which in turn gives rise to a magnetic field. Therefore, due to the motion of ionized gas in the sun, a strong magnetic field is generated (Moldwin, 2008; Echer, 2006 and Howard, 2014). The dynamo action produces intense magnetic fields in the solar atmosphere, which are transported outward to the interplanetary space with the plasma in the solar corona, constituting the solar wind (Hundhauseen, 1972; Kivelson and Russell, 1995).

We think of planets like the Earth as stable, self-contained bodies that do not evaporate into space to a significant extent. Not so with the sun, Moldwin, (2008) and Hargreaves, (1995) defined solar wind as an ionized gas (plasma) and magnetic field which is continuously expelled from the sun. Near Earth, the solar wind is basically a proton–electron gas that flows from the sun (and outward to the entire solar system), with a velocity typically around 400–500 km/s, density around 5 cm^3 and interplanetary magnetic field strength of 5 nT. Other characteristics of the solar wind, such as density, composition, and magnetic field strength, among others, vary with changing conditions on the Sun. Besides solar wind, the interplanetary space is permeated in solar activity transients, e.g., the remnants of solar flares, coronal mass ejections (CME).

1.2 Interplanetary magnetic field (IMF**)**

The region between the sun and the planets has been named the interplanetary medium. Although in the past it was considered a perfect vacuum, since the beginning of the 1960s it is known to be a turbulent region dominated by the solar wind (Echer et al. 2006). Therefore, the part of the sun's magnetic field that is pulled out into the heliosphere by the solar wind is called the interplanetary magnetic field (IMF) (Moldwin, 2005). Its characteristic spiral configuration when viewed from above or below the equatorial plane is due to the sun's rotation. The interplanetary magnetic field is a vector quantity with a three-axis component as shown in Figure 1, two of which (Bx and B_y) are oriented parallel to the ecliptic. The third component, the B_z value is perpendicular to the ecliptic.

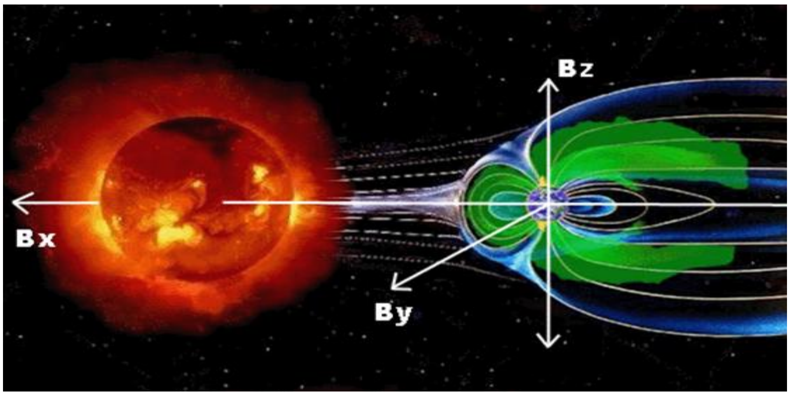

Figure 1: Vector components of interplanetary magnetic field interaction with Earth's magnetosphere (www.spaceweatherlive.com)

In the solar-magnetosphere interaction, the B_z component of the arriving solar wind thus acts as an on/off switch. The Earth's magnetic field is northward directed (has a positive B_z). Thus, when the interplanetary magnetic field of the solar wind is southward directed (negative B_z) then the field lines of IMG and the Earth's magnetosphere interconnect, distorting the Earth's dipole field and providing entry for the solar-wind particles into the magnetosphere. The southward turning IMF becomes the critical requirement for initiation of major magnetic disturbances at Earth magnetosphere (Campbell, 2003).

1.3 Earth's Magnetosphere

This is a region of space surrounding Earth and dominated by Earth's magnetic field. The magnetosphere is in constant interaction with solar wind which delivers charged particles depending on its direction and magnitude. The bow shock, magnetopause, magnetotail are the outer regions of the magnetosphere, while the plasmasphere, Van Allen radiation belt and the ring current characterized by the population of charged particles form the inner regions of the magnetosphere as shown in figure 2. One commonly distinguishes four kinds of electric currents in the magnetosphere (Maltsev and Ostapenko, 2000): 1) the magnetopause currents; 2) the ring current formed by energetic particles trapped at distances from about 3 to 7 R_E (R_E is the Earth radius); 3) the magnetotail current; and 4) the field-aligned currents.

The magnetopause is a surface boundary between the magnetosphere (planet's magnetic field) and the surrounding plasma (solar wind). It moves inward and outward as the solar wind intensity increases and decreases, i.e. compressed on the dayside and elongated on the nightside. This interaction between the magnetosphere and solar wind creates the magnetopause current. Intensification of this current can be observed during a sudden storm commencement (initial phase) in geomagnetic storms when IMF B_z is southward and impulse when IMF B_z is northward. The magnetotail is an elongated region of the magnetosphere that extends in the opposite direction from the sun. The magnetotail is a reservoir of magnetic energy that powers several magnetospheric processes. The magnetotail is subject to global instabilities that produce "substorms," which are surges of Earthward convection that occur on average a few times per day (Borovsky & Valdivia, 2018). Field aligned currents are currents that flow along geomagnetic field lines, caused by the spiralling of electric charges around magnetic field lines. They connect the magnetosphere currents with ionosphere currents, transferring energies that cause auroras and ionospheric disturbances. The ring current flows around the Earth due to the drift of positive ions (westward) and electrons (eastward), with the shape of a ring. It is at a distance of $\sim 3 - 8\ R_E$ and lies on the equatorial plane. Intensification of this current leads to the decrease of the ground measured horizontal component (H) of the geomagnetic field during geomagnetic storms.

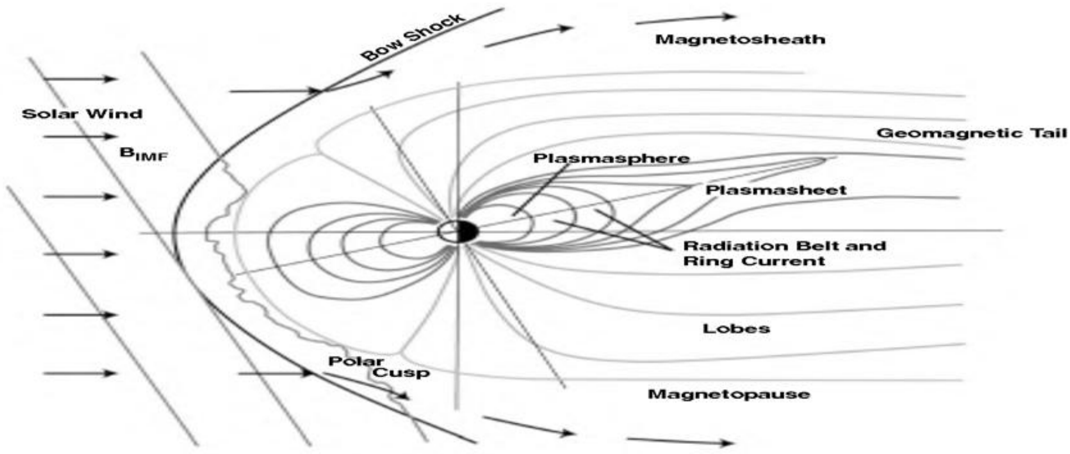

Figure 2: Cross section of Earth's magnetosphere (Campbell, 2003)

1.3.1 Geomagnetic Storm

The geomagnetic storms are the disturbances of the Earth`s magnetic field and the impact of solar wind particles enhancement (Buonsanto, 1990; Gonzalez et al., 1994; Kumar and Kumar, 2019). They are produced when the interplanetary magnetic field (IMF) B_z component turns southward, strengthens (IMF $B_z < -10nT$), and remains southward for substantial length of time (longer than ~3hr; Gonzalez et al., 1994; Gonzalez & Tsurutani, 1987).

The main solar sources of geomagnetic disturbances are coronal mass ejections and high-speed solar wind streams from coronal holes. These sources are associated with different types of magnetic fields on the sun and their contributions to geomagnetic activity strongly depend on the 11-year solar cycle (Legrand & Simon, 1981). The clouds of plasma ejected from the solar corona are coronal mass ejections (CMEs) and they travel outward from the sun carrying an embedded magnetic field. CMEs are most frequent at solar maxima and their contribution to geomagnetic activity is most pronounced in this period. Another solar source of geomagnetic disturbances is high-speed solar wind streams originating from coronal holes. Coronal holes are large dark regions in the solar corona as observed in extreme ultraviolet and soft X-rays. They are characterized by low plasma density and temperature. The interaction of high-speed streams with solar wind results in the formation of co-rotating interaction regions (CIR) with compressed magnetic fields. The co-rotating high-speed streams become more frequent during a declining phase of the solar cycle, so their contribution to geomagnetic activity increases in this period (Veretenenko et al., 2020).

The ring current in Earth's magnetosphere characterized by high energy particles gives rise to a magnetic field that points in the opposite direction to the dipole field at Earth's surface. A magnetic index, called the disturbed storm time index (or Dst), measures the deviation or change in Earth's magnetic field from its normal quiet time value, the strength of Earth's internal magnetic field. When this index goes negative (indicating a decrease in the ground measured Earth's magnetic field), it is due to intensification or increase in the strength of the ring current (Moldwin, 2008; Gonzalez et al. 1994). A schematic geomagnetic storm (Figure 3) can be divided into the initial phase, main phase and recovery phase. The initial phase is caused by an enhancement of solar wind behind the shock wave. It is a quasi-steady state preceded by sudden storm commencement. The main phase of the geomagnetic storm is characterized by the decrease in the horizontal (H) component of the geomagnetic field. The recovery phase actively follows the main phase and is characterized by a slow return of H field back to pre-storm level. Geomagnetic storms can be subdivided into sudden and gradual storms depending on whether a sudden storm commencement (SSC) was observed at the onset of the storm or not. Sudden geomagnetic storms (SG- storms) are characterized by a clear SSC, while gradual geomagnetic storms (GG-storms) do not exhibit SSC. The increase of Dst during SSC phase is due to the intensification of the magnetopause current cause by the compression of the magnetosphere by the solar wind of high pressure and velocity. Table 1.1 shows the definition of geomagnetic activity levels based on the Dst index.

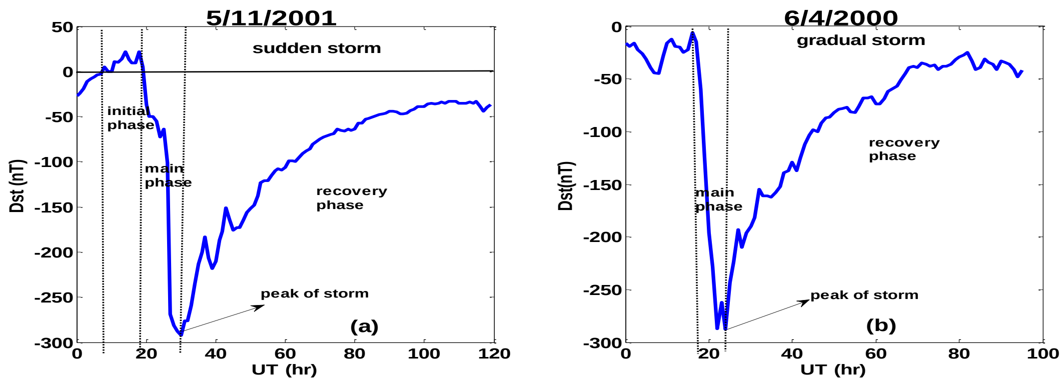

Figure 3: Classical sudden (left) and gradual (right) geomagnetic storms.

Table 1: Definition of geomagnetic activity intensity levels (Echer et al., 2006)

Level	Dst, (nT)
Intense	Dst ≤ -100
Moderate	-50 ≥ Dst < -100
Weak	-30 ≥ Dst < -50
Quiet	Dst > -30

1.4 Ionosphere

Earth's atmosphere can be divided into a series of layers. Each layer may be defined in several ways: the air temperature varies through it, by the gases that comprise it, or even by its electrical properties (Donald, 2009). Figure 4 shows the vertical layers of the atmosphere as related to temperature profile.

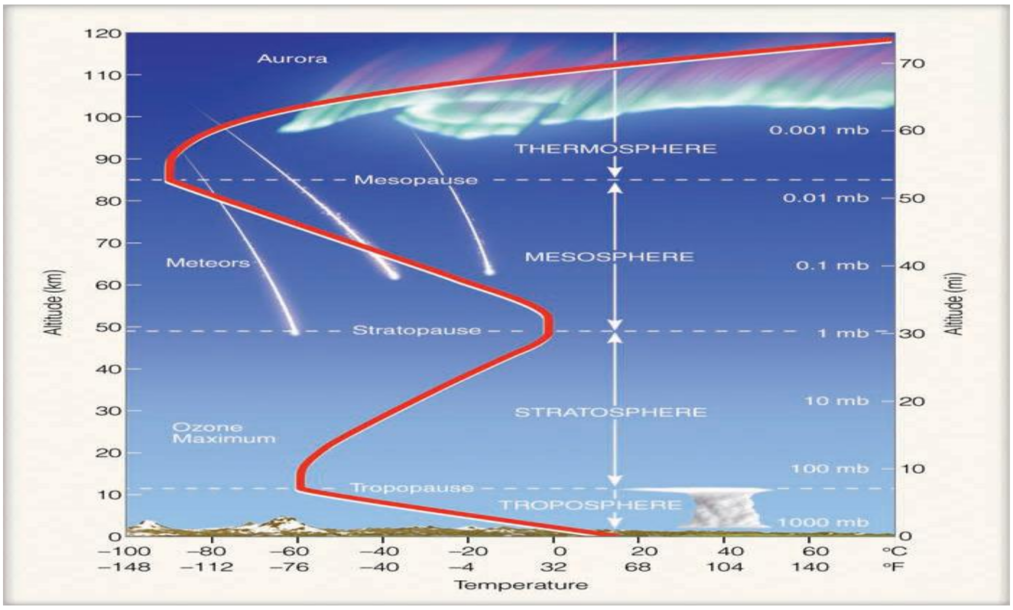

Figure 4: Layers of the atmosphere as related to the average profile of air temperature above the earth's surface (Donald, 2009).

The ionosphere is not really a layer, but rather a region within the upper atmosphere where large concentrations of ions and free electrons exist. Ions are atoms and molecules that have lost (or gained) one or more electrons. Atoms lose electrons and become positively charged when they cannot absorb all the energy transferred to them by a colliding energetic particle or the sun’s energy. The plasma concentration in the ionosphere involves a production and loss process. The production processes involve photochemical absorption of solar radiation from the sun and the loss processes involve ion species recombination in the absence of solar radiation. Specifically, the ionosphere is divided into *D*, E, F1, and F2 layers which are distinct only in the daytime ionosphere. At night, the ionosphere has only the E and F layers as the D layer disappears, the E layer is weakened and the F1 layer is combined with the F2 layer to form the F layer.

To study the ionosphere, a special observatory instrument is used to monitor the changing ionospheric height-frequency profile from which electron density profiles can be determined. This instrument, which generates and receives a broad range of radio-wave frequencies, determines the reflection height from the delay time between an upward-directed specific frequency transmission and the corresponding down-coming return signal reception. Electron densities are exactly computed from the radio-wave frequency using special refraction formulas. The reflected frequency varies in a way similar to the square root of the electron density. The instrument "sounds" the ionosphere, hence the name *ionosonde*. Satellite instruments for a similar function, but which probe the ionosphere below their orbit, are called "topside sounders." A measure of the number of electrons of the ionosphere in a unit cross-section column above an observatory is called the total electron content (TEC) of the site at a particular time. The limiting value of a transmitted radio-wave frequency at which reflections just begin to disappear from any specific region is called the critical penetration frequency, f0, of that region (e.g., f0F2 for the critical frequency of the F2 region). Associated with each critical frequency is a peak density (NmE, NmF1, NmF2) and a peak height (hmE, hmF1, hmF2), which is the altitude of the density maximum (Campbell, 2003; Schunk & Nagy, 2009). Figure 5 shows the variation of the ionospheric layers with height and density of electrons. Solid curves give the electron densities; the scale is at bottom. Long-dashed curves indicate the estimated regional density contribution. N2, O2, NO, O, H, and He represent atomic, molecular, and +ion composition. Ionospheric regions are named, from the bottom up, D, E, F 1, and F 2. Radio-wave soundings near the region maxima are illustrated with short dashes

Studies by various researchers reveal that the total electron content of the F2-layer ionosphere varies with local time, season and geomagnetic latitude. Photo-production, chemical loss, and transport by thermal expansion, neutral winds, waves, tides and electric fields of internal and external origin which are processes that govern the ambient ionosphere, also act during periods of disturbance. The modified magnitudes, phases and time-constants of those processes blend in different ways during each storm, and thus the challenge facing current research is to characterize such effects correctly and to implement them into current models.

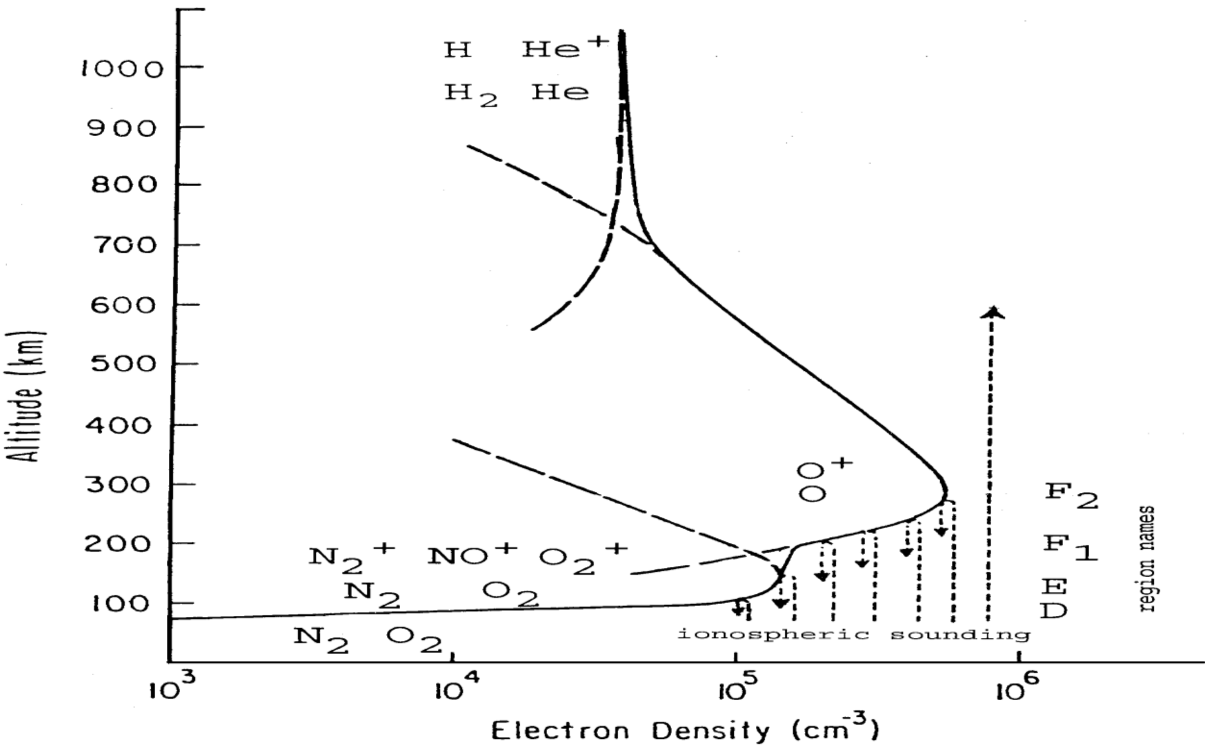

Figure 5: Typical summertime composition of Earth's ionosphere (Campbell, 2003)

1.5 Ionospheric Storm

It shows the critical frequency of F2-layer (f_0F_2) or total electron content (TEC) changes. The large decrease of f_0F_2 or TEC is the ionospheric negative storm and the significant increase of f_0F_2 or TEC is referred to as positive storms (Fagundes et al., 2016; Maruyama et al., 2004). Figure 6 and 7 show examples of positive and negative ionospheric storms respectively (Lekshmi et al, 2011). Following the main phase onset (MPO) at around 09 LT (=UT + 9 hrs) on 22 October the storm-time Nmax (solid curve) remains much greater than the seven quiet-day average prior to the storm (dashed curve) in figure 6. For figure 7, the main phase onset (MPO) at around 04 LT (=UT+9 hrs) on 2 October the storm-time Nmax (solid curve) remains much lower than the seven quiet-day average prior to the storm (dashed curve).

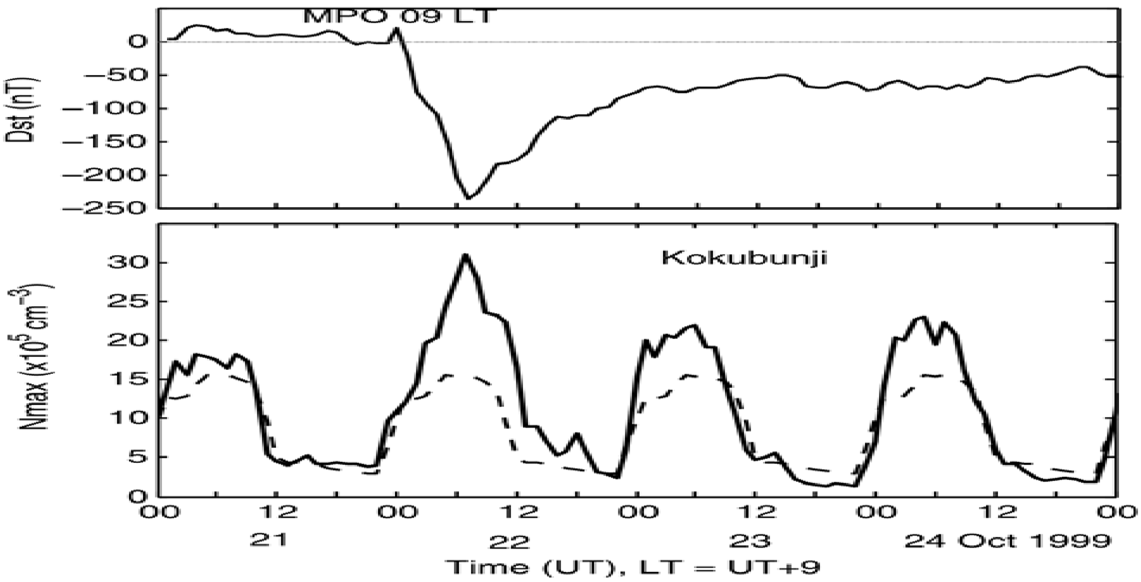

Figure 6: (bottom) Example of a positive ionospheric storm at Kokubunji during (top) the geomagnetic storm of 22-25 October 1999

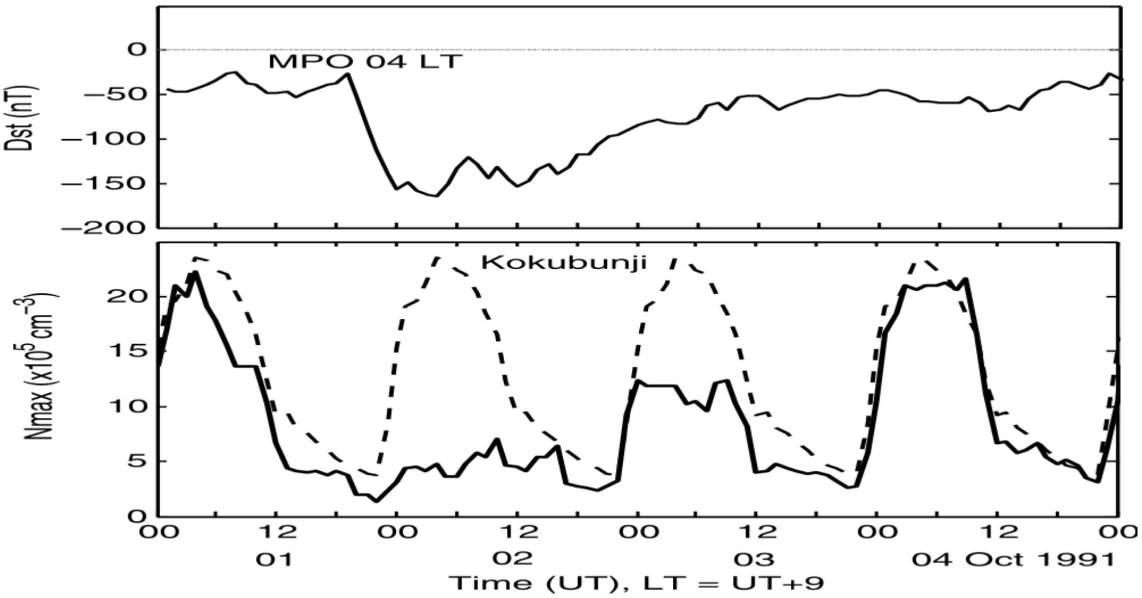

Figure 7: (bottom) Example of a negative ionospheric storm at Kokubunji during (top) the geomagnetic storm of 2-4 October 1991.

In general, F region ionization is positively correlated to the density ratio of atomic oxygen O and the molecular Nitrogen N_2. The joule heating (JH) at high latitude, which could persist for several days is associated with auroral electric currents and generates storm-time thermospheric neutral winds with decreased O/N_2 density ratio and gravity waves, which can generate travelling atmospheric disturbances (TADs) and travelling ionospheric disturbances, TIDs, (Balan et al., 2011; Habarulema et al., 2015). TADs/TIDs flow to middle and low latitudes, which, along with phenomena as the prompt penetration of electric field (PPEF; Huang et al., 2005) and the disturbance dynamo electric field (DDEF; Blanc & Richmond, 1980, Fejer, 2011; Scherliess & Fejer, 1997), mainly change the dynamics and composition of both the ionosphere and thermosphere globally, leading to the occurrence of positive/negative ionospheric storm.

The PPEFs are associated with rapid changes in the magnetospheric convection electric fields and are well correlated with the IMF B_z component, whereas DDEFs are associated with the changes in the thermospheric neutral winds pattern. The PPEFs are instantaneous and of short duration (~1-2hr) but under the long duration of IMF B_z southward can last significantly long up to 8-10hr (Huang, 2008) and have the eastward/westward polarity on the day/nightside.

The DDEFs with timescales from a few to several hours but last longer and change slowly. They can affect the low-latitude ionosphere up to a day or two after the onset of the storm and dominate during the recovery phase of the storm. However, the relative contribution of storm-time electrodynamical and compositional changes in the ionosphere varies with location, season, local time, storm phase and its intensity and other factors (Liu et al., 2014).

Ionospheric storm effects vary with latitude, hence opportunities to study the blending of processes are themselves functions of latitude. For example, horizontal convection dominates in the polar caps, auroral particle precipitation and electrodynamics in the auroral zones, while expansions and contractions of the equatorial ionization anomaly (EIA) drive the strongest effects at low latitudes. The interplay between positive and negative storm effects at midlatitudes relates directly to the time constants for the appearance and persistence of three processes: (a) electric fields of magnetospheric origin, (b) equatorward winds from auroral heating, and (c) the O/N_2 changes due to auroral heating. Effects (a) and (b) cause positive phases in NmF2 and TEC, while (c) produces their negative phases. These processes are either increased or decreased towards the poles or low latitude regions. these time-line relationships date at least to the pioneering work of Mendillo (1973) and Balan and Rao (1990).

The study of ionospheric storms offers the opportunity to assess the blending and phasing of mechanisms and, perhaps, advance our understanding of the ambient ionosphere as well. This is possible because ionospheric storms provoke changes in a few days that mimic changes in the ambient ionosphere that occur over far greater time spans, e.g., with seasons or phases of the solar cycle.

1.6 Effects of Ionospheric Storms

The negative ionospheric storms in which the total electron content (TEC) decreases much below its normal level causes serious problems (such as radio block outs) in ground-based HF radio communications. Radio blackout is a prolonged period of fading or faded radio communications, primarily in the high frequency range (3 – 30MHz). This is because of recombination processes which dominate negative ionospheric storms, thereby decreasing the density of ionized particles in the ionosphere.

Also, positive ionospheric storms in which TEC increase much above their normal levels can cause serious problems (such as time delay, range error and scintillations) in satellite communication and navigation. Through both refraction and diffraction, the ionosphere alters the apparent speed and direction of the signal. This causes an apparent delay in the signal's transit from the satellite to the receiver during positive ionospheric storms (Balan et al. 2011).

1.7 Purpose of the Study

The purpose of my PhD project is to study the variation of total electron content (TEC) during geomagnetic storms at the West-European middle latitudes: Iberian Peninsula and Portuguese archipelagoes of Azores and Madeira.

The preliminary study presented here is the first stage of my PhD project and is aimed at the statistical analysis of the variation TEC caused by geomagnetic storms. It contains

(i) a study of TEC variations during geomagnetic storms in relation to the local time, the seasons, the severity of the geomagnetic storms, the type of storms (sudden or gradual) and the phase of the solar cycle.

(ii) identification of positive, negative ionospheric storms and estimate their strength during geomagnetic storms.

(iii) estimation of the standard deviation of the measured TEC.

CHAPTER TWO

LITERATURE REVIEW

2.1 Variations of ionospheric storms with latitudes, seasons, local time, severity and type of storm

Matsushita (1959) and Mendillo (2006) gave a comprehensive summary of TEC storm phenomenon, both in defining TEC morphology patterns as well as in identifying all the physical drivers of F layer storm effects. All the known characteristics of global F region storms were revealed as follows: (1) the positive phase lasts longer and becomes more prominent with decreasing latitude, followed by a prolonged negative phase that is stronger with increasing latitude. (2) when the positive phase has a noticeable local time component, its maximum amplitude occurs near 18:00 LT (local time) at sub auroral latitudes (3) the influence of season is that positive storms are more pronounced in winter and negative storms are more pronounced in summer.

The reason for these latitudinal variations in the positive phase is due to the two dominant currents towards the equator and the poles. These are the equatorial ionization anomaly (EIA) and auroral currents which cause an increase in the production of ions and subsequent enhancement of plasma in the ionosphere during geomagnetic storms. This is because of the varying effects of the PPEF which affects mainly the positive phase of ionospheric storms and DDEF whose effect is noticed during the recovery phase. For the prolonged recovery of the negative phase, it shows that more ions are been injected at higher latitudes hence the longer time it takes for recombination process during the recovery phase of geomagnetic storms. For the maximum amplitude at 18:00 LT at sub auroral latitude, it is as result of increase in the production of ions prior to this time. At midday, when the solar radiation is maximum, the ionosphere is highly ionized. Hence, when there is an increase in plasma from geomagnetic storms around dusk, it enhances the number of already ionized electrons, depicting the positive phase during ionospheric storms. The seasonal effects of storms occur due to the hemispheric difference in seasonal anomaly. Specifically, the winter F-layer has larger daytime NmF2 and TEC than in summer in both hemispheres, but the effect is far more robust in the Northern hemisphere, an effect called the hemispheric asymmetry (Rishbeth and Mueller-Wodang, 2006). These mechanisms for the positive phase act upon higher plasma densities in the Northern Hemisphere and produce very large dusk effects during winter.

Consequently, while studying 206 geomagnetic storms classified into sudden (SSCs) and gradual (GSCs) storms commencement, Mendillo & Narvaez (2010) observed seasonal and local time dependence in the signatures of ionospheric storms. These storms occurred in solar cycle 20 between 1964 and 1976. The patterns of the ionospheric storms were classified into three patterns depending on storm commencement (SCs) during different portions of the day. They are characterized by the occurrence or (lack of occurrence) of the afternoon enhancement (dusk effect) of the positive phase.

The patterns are: (a) Regular positive phase (RPP) pattern, for events when the SC occur during daytime hours (b) No positive phase storms, for events when SCs occur during pre-sunrise or early in the day, the ionospheric response exhibits only a negative phase (c) Delayed positive phase, for storms that occur in the post sunset period or very early in the day, the ionospheric response exhibit only a dusk effect on the subsequent afternoon. Also, SSCs and GSCs exhibit quite consistent patterns – with small difference noted for the strength of the dusk effect (larger for GSC events), the depth of the negative phase (larger for SSC events), and duration of the negative phase (a somewhat faster recovery for SSC events).

Furthermore, variations of ionospheric storms were studied with respect to seasons, severity of storms, phase of solar cycle, local time dependence for three sub-auroral (~high midlatitude) stations on different hemispheres, Mendillo & Narvaez (2009). These 206 storms were selected from solar cycle 20 and were observed at three stations (Hobart 42.9ºS 147.3ºE, Wallops Island 37.8º N 75.5ºW and Christchurch 46.3ºS 172.8ºE). The results obtained could be related to seasonal, longitudinal and hemispheric differences. For each of these differences studied, the statistical average of the storms related to the differences were calculated. It was found that the local time of the onset of a geomagnetic storm exerts a strong influence on the occurrence of positive and negative phases for each storm, and that the depth of the negative phase is linked to the severity of the geomagnetic storm. Differences also occur that relate to the phase of the solar cycle in which a storm occurs.

Specifically, Barata et al. (2023) studied TEC variations across the Atlantic Ocean from mainland Portugal to the Azores (~9° W to ~26° W, respectively) and at different latitudes (mainland Portugal and the Azores at ~40° N versus Madeira at ~30° N), through the comparative study of eight geomagnetic storms from 2015 to 2022. Their result reveals that in many cases, the amplitude of TEC variations at Madeira was larger than in the other two locations, probably due to its lower latitude. For some of the storms, there are differences (not just in the amplitude of TEC variations, but in appearance of certain features) in the ionospheric response between the northern (Azores and Lisbon) and southern (Madeira) parts of the studied region. Also, there was no clear dependence between the strength of a geomagnetic storm and the strength and the type of a following ionospheric storm.

Blagoveshchensky et al. (2018) also studied the impact of magnetic storms on the global TEC distribution along three meridians: American, Euro-African and Asian-Australian. Six geomagnetic storms of different intensity: from Dst_{min} = -46nT to Dst_{min} = -223nT were analyzed. For the majority the storms, almost simultaneous occurrence of ΔTEC maximums was observed along all three meridians at the beginning of the storm. The transition from a weak storm to a superstorm (the increase of magnetic activity) almost does not affect the intensity of the ΔTEC maximum. The seasonal effect consists in general dominance of a negative phase (decrease of TEC) in summer and a positive phase (increase of TEC) in winter. To sum up, there was no dependence of ΔTEC maximums among the three meridians on the intensity of magnetic activity.

Variations of ionospheric storms with latitude, season, local time and solar activity were studied by Lekshmi et al. (2011) at Kokubunji (26.8°N magnetic latitude) and Boulder (47.4°N). Results shows a preference of main phase (MP) onset at around UT (universal time) midnight during major (-250 nT < Dst < -100 nT) geomagnetic storms. The number of positive ionospheric storms at Kokubunji (about 250) is more than double that at Boulder as expected from a physical mechanism of the positive storms, due to the enhancement of EIA around the magnetic equator where Kokubunji is located. Also, the occurrence of the positive storms at both stations also shows a preference for the morning-noon (05 – 12 h LT) onset of geomagnetic storms as expected, because of ionization processes dominant in the ionosphere during this time. The occurrence of the negative ionospheric storms follows the solar cycle phases (most frequent at solar maximum) better than the occurrence of positive storms. And finally, the strength of both positive and negative ionospheric storms at both stations shows a weak positive correlation and large scatter with the intensity of the geomagnetic storms, suggesting large variability of the drivers of the ionospheric storms

From the above reviews, there are few studies for locations in Portugal and the Iberian Peninsula. It has been established that TEC of the ionosphere varies with latitudes and longitudes. The work by Barata et al. (2023) did not consider the types of storms: whether they are sudden or gradual storm. Also, the number of storms studied was limited. Although their work has set the basis, further research would be carried out in my PhD project. I am going to select storms in the decreasing phase of solar cycle 24, classify them into GSC and SSC. This phase of solar cycle is worth studying to obtain results of the occurrence of positive and negative storms as compared to the results of Lekshmi et al. (2011). In their work, it was found that negative storms occurred frequently compared to positive storms during maximum phases of solar cycle 22-23. Furthermore, the statistical variations in positive and negative phase of change in TEC would be studied in relation to the phase of solar cycle, seasons and time of occurrence of the geomagnetic storms.

CHAPTER THREE

DATA AND METHODS OF DATA ANALYSIS

3.1 DATA

3.1.1 TEC DATA

The ionospheric TEC data used in this work covers the time interval between January 2015 and December 2019, corresponding to the decreasing phase of solar cycle 24. TEC data were collected at three different Portuguese locations as shown below in table 3.1. These data were accessed from the National Network of Permanent GNSS Stations (ReNEP), a public geo-positioning service provided by the general directorate of Territory, Lisbon (https://renep.dgterritorio.gov.pt/).

Table 2: Coordinates of GNSS Receivers

Location	Latitude	Longitude
Lisbon (Cascais)	38.7ºN	9.14ºW
Azores (Furnas)	37.8ºN	25.4ºW
Madeira (Funchal)	32.7ºN	16.9ºW

The data for each storm event were selected as follows: two days before the storm commencement day, the storm commencement day, day of minimum dst and two days after the day of minimum dst.

Based on seasons, the storms are selected from summer (May, June, July, August), winter (November, December, January, February), Equinox (March, April, May, September, October) months. Table 3.2 below shows the storms selected together with the minimum Dst. Please note that for Lisbon and Madeira LT = UT and for Azores LT = UT – 1 h.

3.2: Selected Table geomagnetic storms

Table 3: Selected table of geomagnetic storms

S/N	Storm dates	SSC (Y/N)?	Storm commencement time UTC	Storm Dst minimum, UTC	Dst min, nT	Kp max	Ionospheric response (type, max amplitude in TECu & SD, synchrony: Y/N)
1.	01.03.2017	Y	01.03.2017 8h	01.03.2017 22h	-62	6-	+ 16-23 TECu (9-13 SD) Y
2.	27.03.2017	Y	26.03.2017 22h	27.03.2017 17h	-71	6+	+ 10-13 TECu (4-5 SD) Y
3.	04.04.2017	N	04.04.2017 6h	04.04.2017 11h	-65	5-	0 Casc&Frns Func - +/- 5 TECu (~ 2.5 SD) N
4.	20.04.2017	Y	19.04.2017 24h	20.04.2017 5h	-54	6-	-/+ 6 -9.8 TECu (3 – 5 SD) Y
5.	21 – 22.04.2017	N	21.04.2017 19h	22.04.2017 9h	-64	6-	+ 6 – 9 TECu (3 – 5 SD) Y
6.	27-28.05.2017	Y	27.05.2017 22h	28.05.2017 8h	-146	6+	-/+ 10 -12 TECu (5 – 6 SD) Y
7.	16.07.2017	Y	16.07.2017 7h	16.07.2017 14hr	-71	6-	+ 16 – 20 TECu (7 – 9 SD) Y
8.	23.08.2017	N	22.08.2017 18hr	23.08.2017 13hr	-52	5-	+ Frns & func 5.8 – 7.5 TECu (2 – 3 SD) N

9.	31.08.2017	Y	31.08.2017 7hr	31.08.2017 12hr	-68	5+	+ 15 – 19 TECu (6 – 8 SD) Y
10.	07-08.09.2017	Y	07.09.2017 2hr	08.09.2017 2hr	-148	8+	+ 9 -14 TECu (3 – 5 SD) Y
11.	16.09.2017	Y	14.09.2017 14hr	16.09.2017 6hr	-71	5+	+ 10 -14 TECu (4 – 6 SD) Y
12.	27-28.09.2017	Y	27.09.2017 6hr	28.09.2017 9hr	-98	7-	+ 10 -12 TECu (4 – 5 SD) Y
13.	12-14.10.2017	N	12.10.2017 2hr	14.10.2017 6hr	-70	5+	+ 10 – 14 TECu (4 – 6 SD) Y
14.	24-26.10.2017	Y	24.10.2017 10hr	26.10.2017 15hr	-51	4-	+ 6 – 14 TECu (2 – 6 SD) Y
15.	07-08.11.2017	Y	07.11.2017 6hrs	8.11.2017 5hr	-82	6-	+ 14 -16 TECu (8 – 10 SD) Y
16.	21.11.2017	Y	20.11.2017 23hr	21.11.2017 7hr	-55	5-	+ 4 – 10 TECu (2 – 6 SD) Y
17.	04-05.12.2017	Y	04.11.2017 9hr	05.11.2017 11hr	-51	5-	+ Casc & frns 4 – 8 TECu (4 – 8 SD) N

3.2 Methods of Data Analysis

Employing the method of analysis in Barata et al. (2023), the following statistical analysis would be carried out in this work.

First of all, a so-called quiet daily TEC variation must be obtained for each of the studied months. To do this the five geomagnetically quietest days of a month was selected from https://wdc.kugi.kyoto-u.ac.jp/qddays/index.html. These are days without geomagnetic disturbances. For each hour (H), from 0 to 23h, the quiet TEC values (TEC_{QD}) are calculated as an average of TEC values for this hour for all quiet days of the month.

$$\overline{TEC_{QD}} = \frac{1}{5}\sum_{i=1}^{5} TEC_i \qquad (3.1)$$

The uncertainties of the quiet TEC values $TEC_{QD}(H)$ were computed using the standard deviation (SD or σ), where TEC_{QD} is the mean of $TEC_{QD}(H)$ for the 24 hours:

$$\sigma = SD = \sqrt{\frac{1}{24}\sum_{H=0}^{23}(TEC_{QD}(H) - \overline{TEC_{QD}})^2} \qquad (3.2)$$

Variations of TEC during geomagnetic storms were studied as differences between the observed TEC and the quiet TEC variation.

$$\Delta TEC = TEC - TEC_{QD} \qquad (3.3)$$

The values of SD were used to determine the values of ΔTEC that was statistically significant. Only ΔTEC values exceeding ±2σ are considered statistically significant.

CHAPTER FOUR

PRELIMINARY RESULTS AND DISCUSSION.

Figures 8 – 10 show the results of the statistical analysis for geomagnetic storms of 1, 2 and 4 from Table 3.2. Each of the figures show plots of Kp, Dst index and ΔTEC.

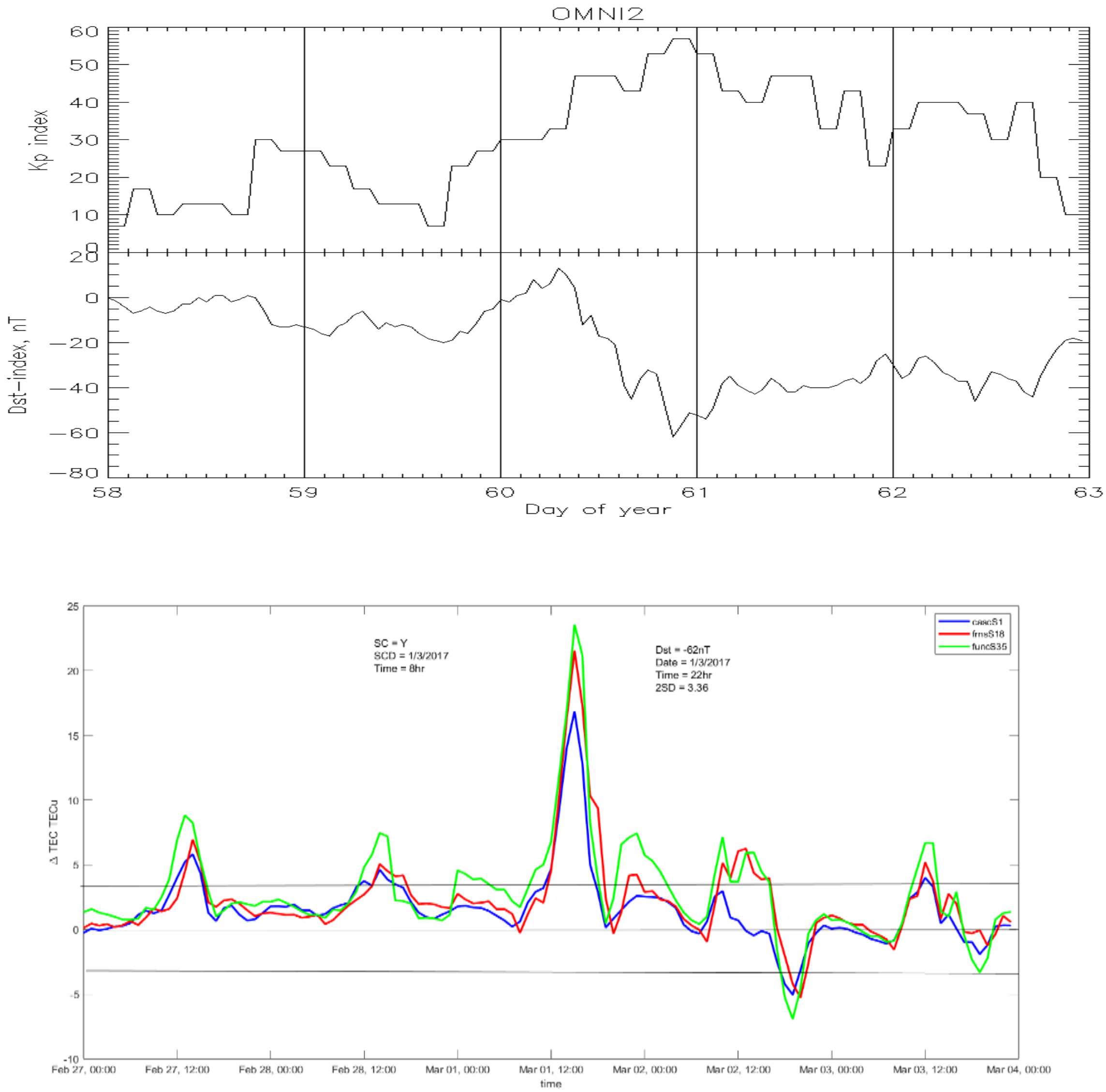

Figure 8: Plots of Dst index (top) and change in TEC (bottom) for 27.02.2017 - 03.03.2017

Figure 8 shows that there was a sudden storm commencement in the morning time (8 h UT) and the Dst minimum in the nighttime (22 h UT) on 01.03.2017 respectively. The ionosphere responded positively to this geomagnetic storm in the afternoon (~ 15 h UT) of 01.03.2017. ΔTEC were above the 2*SD mark, making the results a significant one. The process of ionization which is enhanced during afternoon time in the ionosphere can be said to have caused this peak response in TEC. Other days, before the storm commencement and after Dst minimum also show significant ionospheric responses but low peak values of ΔTEC. The horizontal lines on the positive and negative axis, above and below zero horizontal line, represent 2*SD of ΔTECu respectively. They show the limits above the lines at which an enhancement can be said to be a positive or negative ionospheric storm. Plots in blue, red and green represent ΔTECu variation for Lisbon (Cascais), Azores (Furnas) and Madeira (Funchal) respectively.

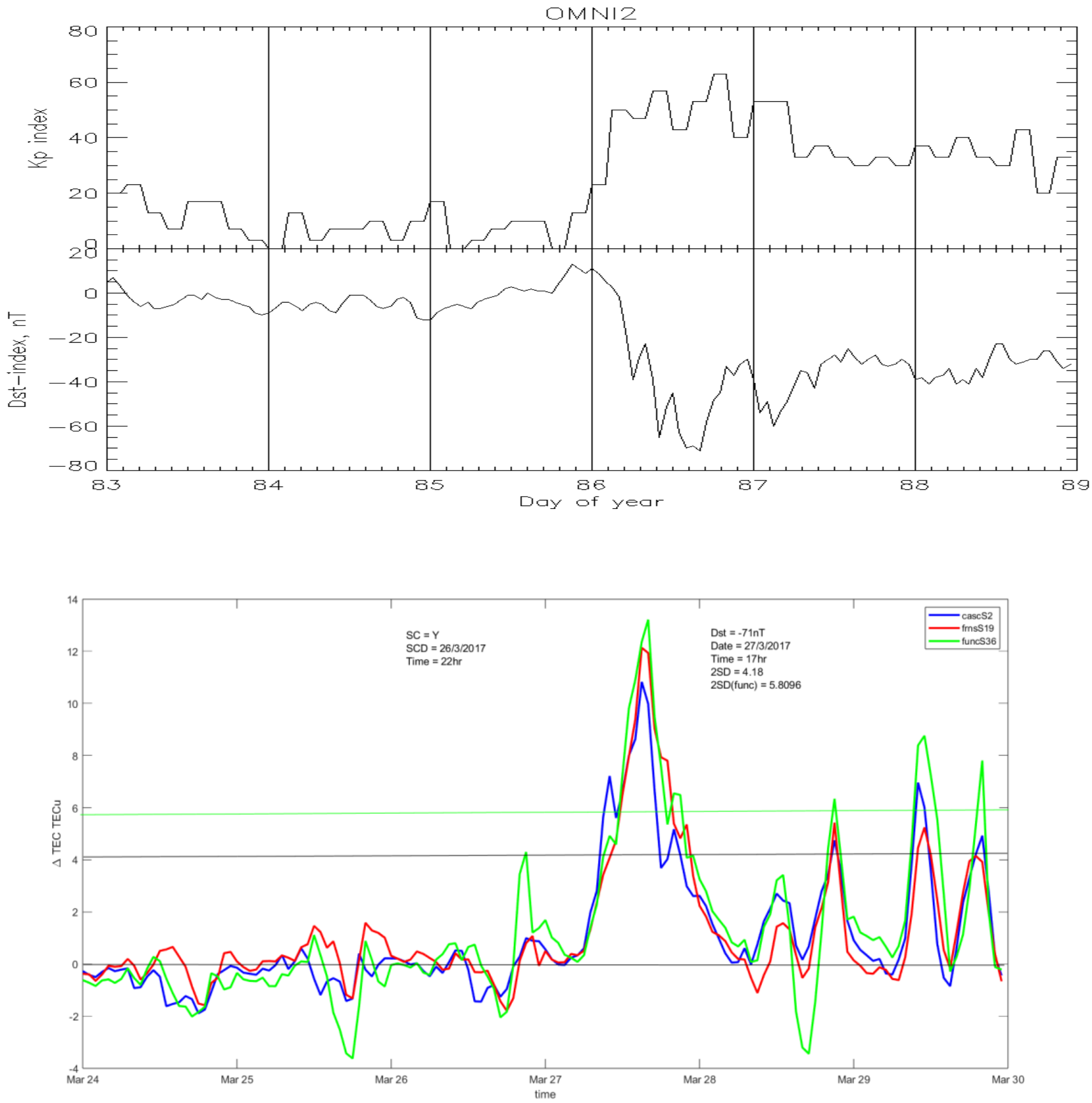

Figure 9: Same as Figure 8 but for 24.03.2017 - 29.03.2017

A sudden storm commencement on 26.03.2017 at 22hr and Dst minimum on 27.03.2017 at 17 h UT characterize the geomagnetic storm of 24.03.2017 – 29.03.2017. The ionosphere in its usual way responded to this geomagnetic storm in the afternoon (~ 15:30 UT) of 27.03.2017, due to ionization processes being enhanced at this time of the day. All the stations response was synchronous and significant above 2*SD.

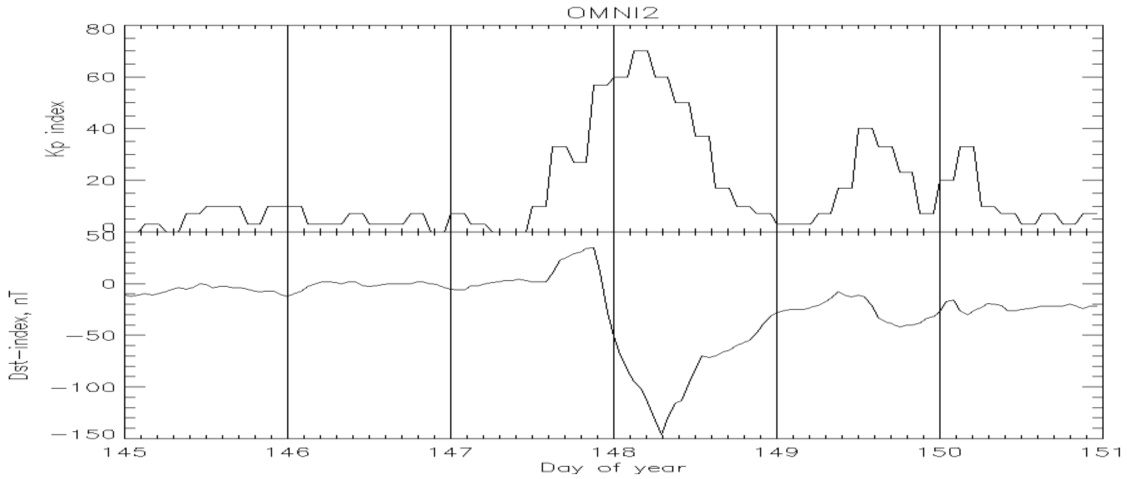

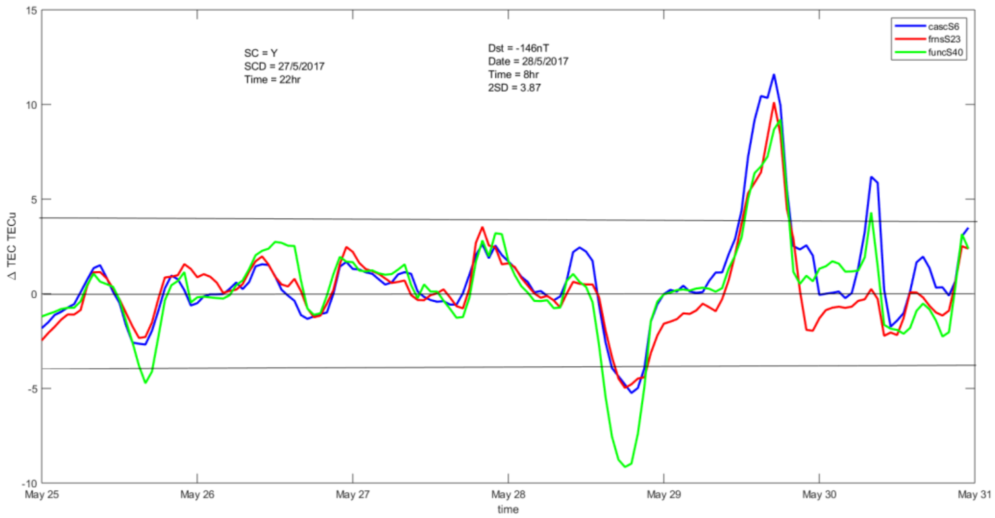

Figure 10: Same as Figure 8 but for 25.05.2017 - 30.05.2017

Figures 10 shows an ionospheric response to a geomagnetic storm which is started with an initial phase on 27.05.2017 (22h UT) with Dst minimum (-146 nT) on 28.5.2017 (8 h UT). There was a significant synchronous negative peak at about 19 h UT on 28.05.2017, with Funchal having the highest peak due to effects of the EIA. This peak ionospheric response occurred after the Dst minimum and during the recovery phase of the storm. There was also another peak of positive synchrony on 29.5.2017 at 17h UT of which Funchal had the highest peak. This second peak was greater than the previous peak even though it occurred two days after the storm commencement. It remains a subject of discussion to see if this type of ionospheric response is common to intense storms whereby its effect can be felt by the ionosphere up to two days after its commencement.

References

Blanc, M., & Richmond, A. D. (1980). The ionospheric disturbance dynamo. Journal of Geophysical Research, 85, 1669–1686.

Balan, N. & Rao, P. B. (1990). Dependence of ionospheric response on the local time of sudden commencement and the intensity of geomagnetic storms, *Journal of Atmospheric & Solar Terrestrial Physics, 52*, 269–275, 1990.

Balan, N., Yamamoto, M., Liu, J. Y., Liu, H., & Lühr, H. (2011). New aspects of thermospheric and ionospheric storms revealed by CHAMP. *Journal of Geophysical Research, 116*, A07305.

Barata, T., Pereira, J., Hernández-Pajares, M., Barlyaeva, T., & Morozova, A. (2023). Ionosphere over Eastern North Atlantic Midlatitudinal Zone during Geomagnetic Storms. *Atmosphere, 14,* 949.

Blagoveshchensky, D.V., Maltseva, O.A., & Sergeeva, M.A. (2018). Impact of magnetic storms on the global TEC distribution. Annales Geophysicae, 36, 1057-1071.

Borovsky, J.E., & Valdivia, J.A. (2018). The Earth's Magnetosphere: A Systems Science Overview and Assessment. *Surveys in Geophysics, 39,* 817 – 859.

Buonsanto, M. J. (1999). Ionospheric storms — *A review. Space Science Reviews, 88,* 563–601.

Campbell, W. H. (2003). *Introduction to geomagnetic fields.* Cambridge University Press, New York.

Chapman, S. (1951). The normality of geomagnetic disturbances at Huancayo. *Pure and Applied Geophysics, 19,* 151-158.

Echer, E., Gonzalez, W.D., & Alves, M.V. (2006). On the geomagnetic effects of solar wind interplanetary magnetic structures. *Space Weather, 4,* 1-11.

Fagundes, P. R., Cardoso, F. A., Fejer, B. G., Venkatesh, K., Ribeiro, B. A. G., & Pillat, V. G. (2016). Positive and negative GPS-TEC ionospheric storm effects during the extreme space weather event of March 2015 over the Brazilian sector. Journal of Geophysical Research: *Space Physics, 121*, 5613–5625.

Fejer, B. G. (2011). Low latitude ionospheric electrodynamics. *Space Science Reviews, 158,* 145–166

Gonzalez, W. D., Joselyn, J. A., Kamide, Y., Kroehl, H. W., Rostoker, G., Tsurutani, B. T., & Vasyliunas, V. M. (1994). What is a geomagnetic storm? *Journal of Geophysical Research, 99,* 5771–5792.

Gonzalez, W.D., & Tsurutani, B.T. (1987). Criteria of interplanetary parameters causing intense magnetic storms (Dst < -100nT). *Planet Space Science, 35*, 1101-1109.

Gonzalez, W. D., Tsurutani, B. T., & Gonzalez, A. L. (1999). Interplanetary origin of geomagnetic storms. *Space Science Reviews, 88,* 529-562.

Hargreaves, J. K. (1995). *The solar terrestrial environment*. Cambridge University Press, Britain.

Howard, T. (2014). *Space weather and coronal mass ejections*. Springer, New York.

Habarulema, J. B., Katamzi, Z. T., & Yizengaw, E. (2015). First observations of poleward large-scale traveling ionospheric disturbances over the African sector during geomagnetic storm conditions. *Journal of Geophysical Research: Space Physics, 120,* 6914–6929.

Huang, C.-S., Foster, J. C., & Kelley, M. C. (2005). Long-duration penetration of the interplanetary electric field to the low-latitude ionosphere during the main phase of magnetic storms. *Journal of Geophysical Research, 110,* A11309.

Huang, C.-S. (2008). Continuous penetration of the interplanetary electric field to the equatorial ionosphere over eight hours during intense geomagnetic storms. *Journal of Geophysical Research, 113,* A11305

Hundhausen, A. J. (1972). Coronal expansion and solar wind. Springer, New York.

Kivelson, M. G., & Russell, C.T. (1995). *Introduction to space Physics*. Cambridge University Press, Britain.

Kumar, S., & Kumar, V. V. (2019). Ionospheric response to the St. Patrick’s Day space weather events in March 2012, 2013, and 2015 at southern low and middle latitudes. *Journal of Geophysical Research: Space Physics, 124,* 584–602.

Lekshmi, D.V., Balan, N., Tulasi R.N, & Liu, J.Y. (2011), Statistics of geomagnetic storms and ionospheric storms at low and mid latitudes in two solar cycles, J. Geophys. Res., 116, A11328.

Legrand, J.P., & Simon, P.A. (1981). Ten cycles of solar and geomagnetic activity. Solar Physics, 70, 173-195.

Vereteneko, S., Ogurtsov, M., & Obridko, V. (2020). Long term variability in occurrence frequencies of magnetic storms with sudden and gradual commencements. Journal of Atmospheric and Solar-Terrestrial Physics, 205(2020), 105295.

Liu, J., Liu, L., Nakamura, T., Zhao, B., Ning, B., & Yoshikawa, A. (2014). A case study of ionospheric storm effects during long-lasting southward IMF Bz-driven geomagnetic storm. *Journal of Geophysical Research: Space Physics, 119*, 7716–7731.

Maltsev, Y.P., & Ostapenko, A.A. (2000). Variability of the Electric Currents in the Magnetosphere. *Physics and Chemistry of the Earth, 25*, 27-30

Maruyama, T., Ma, G., & Nakamura, M. (2004). Signature of TEC storm on 6 November 2001 derived from dense GPS receiver network and ionosonde chain over Japan. *Journal of Geophysical Research, 109*, A10302.

Matsushita, S. (1959). A study of the morphology of ionospheric storms, *Journal of Geophysical Research*, 64, 305–321.

Mendillo, M & Narvaez, C. (2009). Ionospheric storms at geophysically-equivalent sites – Part 1: Storm-time patterns for sub-auroral ionospheres. Annales of Geophysics, 27, 1679–1694

Mendillo, M. (1973). A study of the relationship between geomagnetic storms and ionospheric disturbances at mid-latitudes, *Planet Space Science, 21*, 349–358.

Mendillo, M. (2006). Storms in the ionosphere: Patterns and processes for total electron content, *Reviews of Geophysics, 44*, RG4001

Moldwin, M. (2008). *An introduction to space weather.* Cambridge University Press, Britain.

Rishbeth, H. & M¨uller-Wodarg, I. C. F. (2006) Why is there more ionosphere in January than in July? The annual asymmetry in the F2-layer, Annales Geophysicae, 24, 3293–3311.

Scherliess, L, & Fejer, B. G. (1997). Storm time dependence of equatorial disturbance dynamo zonal electric fields. *Journal of Geophysical Research, 102,* 24,037–24,046.

Schunk, R. & Nagy, A. (2009). *Ionospheres; Physics, Plasma Physics and Chemistry*. Cambridge University Press, New York.